Robust Torque Control of Induction Motor against Variations of Primary and Secondary Resistances

Toshihiko Noguchi, Seiji Kondo and Isao Takahashi

Nagaoka University of Technology
1603-1 Kamitomioka, Nagaoka, Niigata 940-21, JAPAN
Fax: +81-0258-46-6506 Phone: +81-0258-46-6000 E-mail: omom@voscc.nagaokaut.ac.jp

Abstract: This paper proposes new torque control of an induction motor, which is robust against variations of primary and secondary resistances. The control is based on a flux feedback with a flux simulator. The simulator employs a rotor current model so as not to be affected by the variation of the primary resistance, but uses the secondary resistance value to calculate the flux. Its parameter mismatch results in transient phenomena in flux and torque responses. In order to compensate for degradation of the responses, a secondary resistance identifier is introduced into the system. The identifier is perfectly robust against the variation of the primary resistance because it is based on the instantaneous reactive power of the induction motor. To verify the feasibility of this technique, some digital simulations and experimental tests were conducted on the basis of theoretical consideration. The results prove excellent characteristics, which confirms the validity of the proposed scheme.

Introduction

In recent years, field-oriented control has been applied to an induction motor to attain as quick torque response as a dc motor.[1] The control is based on the interaction between flux and torque components of the current. These components can be controlled on the coordinates synchronously rotating with the secondary flux. Therefore it is essential to estimate the flux exactly by using the motor parameters, especially the secondary resistance, whether flux-feedforward-type or flux-feedback-type control is implemented to the system.[2,3] The parameter mismatch of the resistance however, deteriorates both steady-state and transient responses. A number of papers have reported the problem and have explored the means of compensation. It is supposed that the conventional techniques require rather complicated configurations, and seem to have little ability of perfect compensation.[4-6] Some of them use the mathematical model that requires pure integrators or the primary resistance value, which does not enable to obtain the expecting results. Hence it is significant to investigate a new approach.[7,8]

This paper describes a torque control strategy of the induction motor with robustness against the variations of the primary and the secondary resistances.[9] Its principle is based on flux-feedback-type control with a flux simulator and a robust identifier of the secondary resistance. The basic system is originally robust against the variation of the primary resistance, but has high parameter sensitivity of the secondary resistance. The identifier is introduced into the system so as to compensate for the secondary resistance variation perfectly. It is essentially robust against the variation of the primary resistance because it is based on the instantaneous reactive power of the induction motor. In this paper, theoretical consideration is developed, and some computer simulations and experimental tests are described.

Flux and Torque Control of Induction Motor

Configurations of Flux Simulators

An electric-circuit equation and output torque of the induction motor are given on the $\gamma-\delta$ coordinates rotating at an angular speed ω as follows:

$$\begin{bmatrix} v_{1\gamma\delta} \\ 0 \end{bmatrix} = \begin{bmatrix} R_1+(p+j\omega)\ell_2 & (p+j\omega)\dfrac{M}{L_{22}} \\ -\dfrac{R_2}{L_{22}}M & \dfrac{R_2}{L_{22}}+\{p+j(\omega-\omega_m)\} \end{bmatrix} \begin{bmatrix} i_{1\gamma\delta} \\ \psi_{2\gamma\delta} \end{bmatrix} \quad (1)$$

$$T = \frac{M}{L_{22}}\mathrm{Im}\left(i_{1\gamma\delta}\overline{\psi_{2\gamma\delta}}\right) \quad (2)$$

where the variables and the parameters are shown below.

$v_{1\gamma\delta}$: primary voltage vector on the $\gamma-\delta$ coordinates
$i_{1\gamma\delta}$: primary current vector on the $\gamma-\delta$ coordinates
$\psi_{2\gamma\delta}$: secondary flux vector on the $\gamma-\delta$ coordinates
T : output torque
ω : rotating speed of the $\gamma-\delta$ coordinates
ω_m : rotating speed of the rotor
R_1 : primary resistance
R_2 : secondary resistance
L_{11} : primary self inductance
L_{22} : secondary self inductance
M : mutual inductance
$\ell_2 = \dfrac{L_{11}L_{22}-M^2}{L_{22}}$: leakage inductance
p : differential operator
j : imaginary unit
$\mathrm{Im}(x)$: imaginary part of x
$\bar{x}$: complex conjugate of x

The secondary flux $\psi_{2\gamma\delta}$ is derived from the second row in Eq. (1), which can be used as a flux simulator. The simulator is called a rotor current model, and the model requires detecting the primary currents and the rotating speed of the rotor. It is supposed that the model can calculate the flux all over the speed range including zero speed because it does not possess pure integrators. This derivation however, is not practical when ω is a manipulated variable. Therefore the flux has to be calculated on the stator frame or the rotor frame whose rotating speed is known. Assuming that $d-q$ coordinates are on the stator and $\alpha-\beta$ coordinates are on the rotor, the secondary fluxes ψ_{2dq} and $\psi_{2\alpha\beta}$ are derived from the second row in Eq. (1) rewriting the subscripts and replacing ω with the rotating speed of the coordinates.

$$\hat{\psi}_{2dq} = \frac{M}{1+(p-j\omega_m)\frac{L_{22}}{\hat{R}_2}} i_{1dq} \quad (3)$$

$$\hat{\psi}_{2\alpha\beta} = \frac{M}{1+p\frac{L_{22}}{\hat{R}_2}} i_{1\alpha\beta} \quad (4)$$

where $\hat{x}$ represents an estimated or an identified value of x. To calculate primary flux vector $\hat{\psi}_{1dq}$, the leakage flux is added to $\hat{\psi}_{2dq}$ as written in Eq. (5).

$$\hat{\psi}_{1dq} = \frac{M}{L_{22}} \hat{\psi}_{2dq} + \ell_2 i_{1dq} \quad (5)$$

Figure 1 shows the configuration of the flux simulator on each reference frame. The simulator on the $\alpha-\beta$ coordinates has no interference terms to calculate the flux, but it requires coordinate transformation by a rotor position θ_m.

Flux and Torque Control Based on Flux Simulator

Flux-feedback-type field-oriented control

Assuming that γ axis of the $\gamma-\delta$ coordinates is in the same direction as $\psi_{2\gamma\delta}$, ω equals the rotating speed of $\psi_{2\gamma\delta}$. Additionally, assuming constant flux-amplitude control, $i_{1\gamma\delta}$ is expressed as shown below by using the second row of Eq. (1) and Eq. (2).

$$i_{1\gamma\delta} = i_{1\gamma} + j i_{1\delta} = \frac{1}{M}|\psi_2| + j\frac{L_{22}}{M}\frac{T}{|\psi_2|} \quad (6)$$

where $|\psi_2|$ represents amplitude of the flux, and the differential term of $|\psi_2|$ is supposed to be zero because of the constant flux-amplitude control. On the $\gamma-\delta$ coordinates which rotate synchronously with $\psi_{2\gamma\delta}$, the flux amplitude and the output torque can be controlled by manipulating the flux component $i_{1\gamma}$ and the torque component $i_{1\delta}$ respectively. Figure 2 shows a block diagram of field-oriented control based on the flux simulator. As it is necessary to control each component of the current, detected currents and voltage references are transformed by using $\hat{\psi}_{2dq}$ which is calculated in the flux simulator.

$$i_{1\gamma\delta} = \frac{\hat{\psi}_{2dq}}{|\hat{\psi}_2|} i_{1dq} \quad (7)$$

$$v_{1dq}^* = \frac{\hat{\psi}_{2dq}}{|\hat{\psi}_2|} v_{1\gamma\delta}^* \quad (8)$$

Therefore if the simulator calculates $\hat{\psi}_{2dq}$ with an error, current control on the $\gamma-\delta$ coordinates can not be carried out perfectly. This prevents the system from controlling the flux and the output torque without transient phenomena.

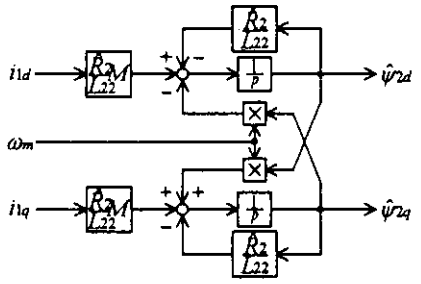

(a) $d-q$ coordinate model.

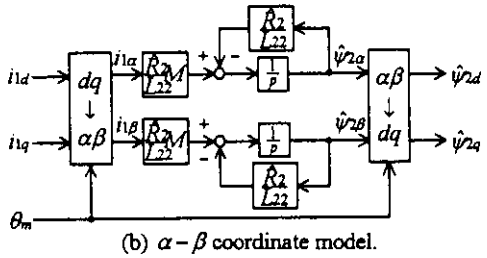

(b) $\alpha-\beta$ coordinate model.

Fig. 1. Configurations of the flux simulators.

Direct torque control based on primary flux

Figure 3 shows a block diagram of the control which has been proposed by the authors.[10] The configuration does not possess current loops but flux and torque loops, and the control is based on their limit cycle operations. Using hysteresis elements in the loops, the optimal inverter-switching mode is selected according to the combination of their outputs. Therefore the flux and the output torque of the induction motor can be controlled directly by the inverter. The primary flux $\hat{\psi}_{1dq}$ is calculated as a feedback signal by using the flux simulator. The simulator has to calculate $\hat{\psi}_{1dq}$ without any errors so that the system can select the appropriate inverter-switching mode as described above.

Effects of Resistance Variations on Flux and Torque Responses

A digital simulation was examined on the control system which was shown in Fig. 2 as an example. The parameters of the induction motor are shown in Table 1, and its output torque was controlled under the condition of a constant rotating speed. Figure 4 shows the step torque responses, whose conditions are described in their captions respectively.

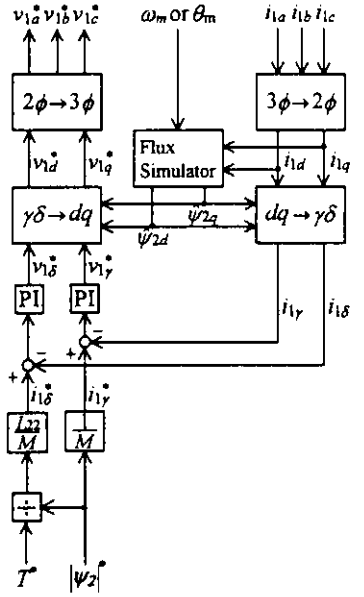

Fig. 2. Block diagram of field-oriented control.

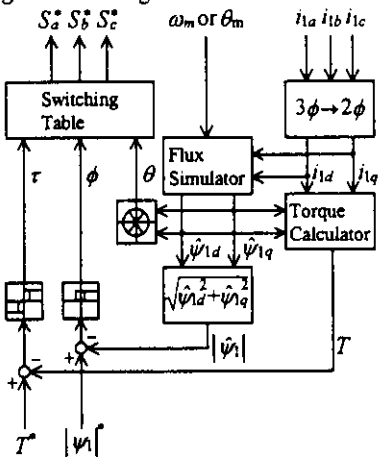

Fig. 3. Block diagram of direct torque control.

As shown in Figs. 4(a) and 4(b), a quick torque response was obtained without any transient oscillation and steady-state errors. It can be stated that the variation of R_1 has no influence on the flux and the torque responses from these results. Therefore the system is essentially robust against the variation of R_1. The reason is that R_1 exists in the current loop as a forward element, and the loop gain compresses the effect of its variation. On the other hand, the parameter mismatch of $\hat{R}_2$ in the flux simulator causes transient phenomena in both flux and torque responses. Figures 4(c) and 4(d) show degradation of the responses. It is found that the parameter mismatch of $\hat{R}_2$ has to be compensated without any relations with R_1 to improve the responses.

It was confirmed that the direct torque control also resulted in the almost same way as Fig. 4. The control is essentially robust against the variation of R_1, but has very high parameter sensitivity of $\hat{R}_2$. It is necessary to compensate for the parameter mismatch of $\hat{R}_2$ in the flux simulator without relations with R_1.

Compensation of Secondary Resistance Variation

Principle of Secondary Resistance Identification

In what follows, a strategy to compensate for the variation of the secondary resistance is derived by introducing the instantaneous reactive power of the induction motor. It is defined as Eq. (9) on the $d-q$ coordinates.

$$Q = \mathrm{Im}\left(v_{1dq}\overline{i_{1dq}}\right) \tag{9}$$

This quantity is a scalar which is calculated statically by using the detected primary voltages and currents. It always gives a true value because no parameters of the induction motor are used.

Replacing the first row of Eq. (1) with the equation represented on the $d-q$ coordinates, and substituting it into Eq. (9), Q can be rewritten as follows:

$$Q = \mathrm{Im}\left(\mathrm{p}\,\psi_{1dq}\overline{i_{1dq}}\right) \tag{10}$$

The term of R_1 in the first row of Eq. (1) is canceled out perfectly in this derivation. Therefore Eq. (10) has no parameter sensitivity of R_1.[4] Equation (10) requires ψ_{1dq}, which may be calculated in the flux simulator. The simulator however, uses the value of the secondary resistance as described before. Equation (10) possibly has an error owing to the secondary resistance variation; hence it is feasible to replace Eq. (10) with Eq. (11).

$$\hat{Q} = \mathrm{Im}\left(\mathrm{p}\,\hat{\psi}_{1dq}\overline{i_{1dq}}\right) \tag{11}$$

where $\hat{\psi}_{1dq}$ is given by Eq. (5).

The difference between Eq. (10) and Eq. (11) can be derived by using Eq. (3) and Eq. (5).

$$\begin{aligned}\Delta Q &= \mathrm{Im}\left\{\mathrm{p}\left(\psi_{1dq}-\hat{\psi}_{1dq}\right)\overline{i_{1dq}}\right\} \\ &= \mathrm{Im}\left\{\mathrm{p}\left(\psi_{2dq}-\hat{\psi}_{2dq}\right)\overline{i_{1dq}}\right\}\end{aligned} \tag{12}$$

This equation represents that the parameter mismatch of $\hat{R}_2$ in the flux simulator results in the error ΔQ. The variation of the secondary resistance is supposed to be very slow compared with electrical time constants. Therefore it is enough to consider a steady state, and the instantaneous variables can be replaced as $\mathrm{p}\rightarrow \mathrm{j}\omega$, $\psi_{2dq}\rightarrow \Psi_2$, $\hat{\psi}_{2dq}\rightarrow \hat{\Psi}_2$ and $i_{1dq}\rightarrow I_1$ in Eq. (3) and Eq. (12), where the upper-case variables represent phasors in the steady state. Then ΔQ is calculated as follows:

$$\Delta Q = \frac{M^2}{L_{22}}\frac{\omega(\omega-\omega_m)^2\left(\frac{L_{22}}{\hat{R}_2}-\frac{L_{22}}{R_2}\right)\left(\frac{L_{22}}{\hat{R}_2}+\frac{L_{22}}{R_2}\right)}{\left\{1+(\omega-\omega_m)^2\left(\frac{L_{22}}{\hat{R}_2}\right)^2\right\}\left\{1+(\omega-\omega_m)^2\left(\frac{L_{22}}{R_2}\right)^2\right\}}|I_1|^2 \tag{13}$$

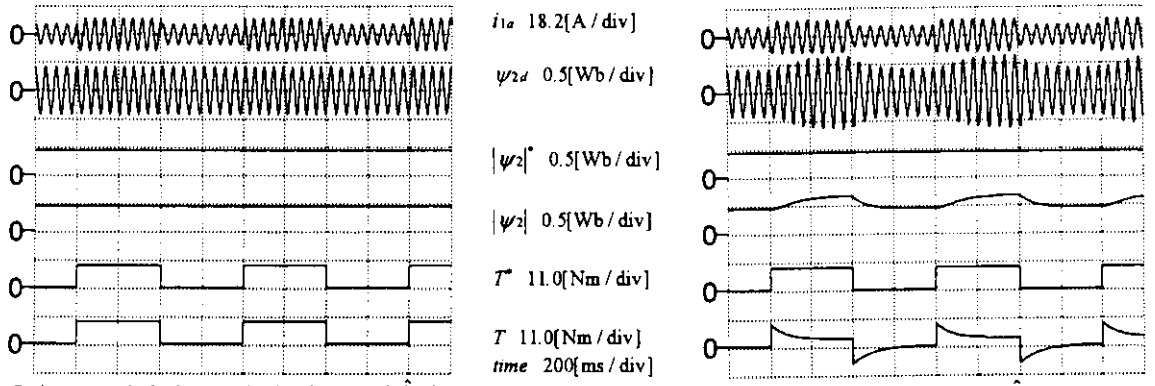

(a) R_1 is not varied (the nominal value), and $\hat{R}_2$ has no parameter mismatch (the nominal value).

(c) R_1 is not varied (the nominal value), but $\hat{R}_2$ has parameter mismatch by 14[%] of the nominal value.

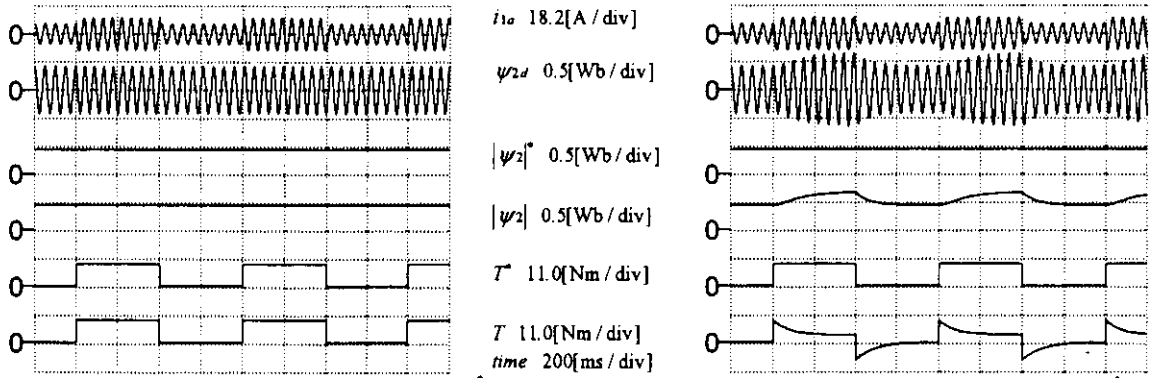

(b) R_1 is varied by 321[%] of the nominal value, but $\hat{R}_2$ has no parameter mismatch (the nominal value).

(d) R_1 is varied by 321[%] of the nominal value, and $\hat{R}_2$ has parameter mismatch by 14[%] of the nominal value.

Fig. 4. Effects of the resistance variations on flux and torque responses (simulation results).

It is recognized that ΔQ is zero if and only if $\hat{R}_2 = R_2$ except the cases of $\omega = 0$ and $\omega - \omega_m = 0$. In other words, it is possible to identify the secondary resistance value uniquely by using ΔQ except the condition of dc-exciting or no-load.

Figure 5 shows a block diagram of the secondary resistance identifier, which is robust against the variation of the primary resistance. The identifier is based on a parallel-type model reference adaptive system. Q of Eq. (9) is a process, and the flux simulator and $\hat{Q}$ of Eq. (11) constitute a mathematical model. The difference between Q and $\hat{Q}$ is used to adjust $\hat{R}_2$ in the flux simulator dynamically. An integrator is employed as an identification algorithm because of a slow variation of the secondary resistance as mentioned before. If the case of $\omega = 0$ or $\omega - \omega_m = 0$ occurs, the identification algorithm holds the value which has been integrated as $\hat{R}_2$, and it does not diverge.

The proposed compensation technique is applied to the flux-feedback-type control with the flux simulator whether it employs the field-oriented control or the direct torque control.

Compensation Characteristics of Secondary Resistance Variation

Figure 6 shows some simulation results of step torque responses with compensation of the secondary resistance variation. These simulation results were obtained under the same conditions as those of Fig. 4. The conditions are described in the captions of Fig. 6.

The initial value of $\hat{R}_2$ was 14[%] of nominal value in each simulation. It was found that the identifier did not operate at no-load condition, and the initial value was held as $\hat{R}_2$. This condition corresponded to the case of $\omega - \omega_m = 0$ in Eq. (13). As soon as the torque reference was applied, the identification started automatically. Transient phenomena were observed at the beginning of the identification because of the parameter mismatch of $\hat{R}_2$. The identified value $\hat{R}_2$ however, converged to the true value in 400[ms], and the flux and the output torque followed their references accordingly. Then excellent torque response was attained without the parameter mismatch because $\hat{R}_2$ had converged to the true value. As shown in Fig. 6(b), the compensation of the parameter mismatch was performed even if the primary resistance varied.

Experimental System and Results

Outline of Experimental System

Some experimental tests were carried out to confirm the feasibility of the proposed scheme. Figure 7 shows a developed experimental system. The system consists of an inverter fed induction motor and a chopper fed dc motor. The parameters of the induction motor are same as those shown in Table 1. Flux and torque control is based on the block diagram shown in Fig. 2.

A fully digitized software control system was developed for the induction motor. The control and the identification processes are completely based on DSP (TMS320C25), and the flow chart of its program is shown in Fig. 8. The program is proceeded in 103[μsec] for every control period. The PWM circuit also employs fully digitized hardware, whose carrier frequency is 5[kHz]. The output torque of the induction motor is controlled by the system without a speed loop.

A load of the induction motor is the dc motor system which has both current and speed loops to keep the mechanical rotating speed constant. The controller is composed of analog hardware for the most part. The shafts of the two motors are coupled with a distortion-gage-type torque pickup.

Experimental Results

To verify the effect of the secondary resistance variation at first, the torque response was examined under the condition of fixed $\hat{R}_2$. Figure 9 shows step responses of 100[%] torque. The conditions of the tests are described in the captions of Fig. 9.

As shown in Fig. 9, the torque component of the current $i_{1\delta}$ followed its reference $i_{1\delta}^*$ quickly, and had no overshoot. Transient phenomenon in the torque response however, was observed in Fig. 9(a) because of the parameter mismatch of $\hat{R}_2$. On the other hand, the ideal torque response was successfully

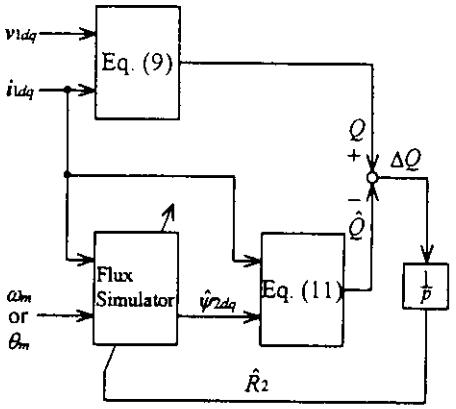

Fig. 5. Block diagram of the secondary resistance identifier.

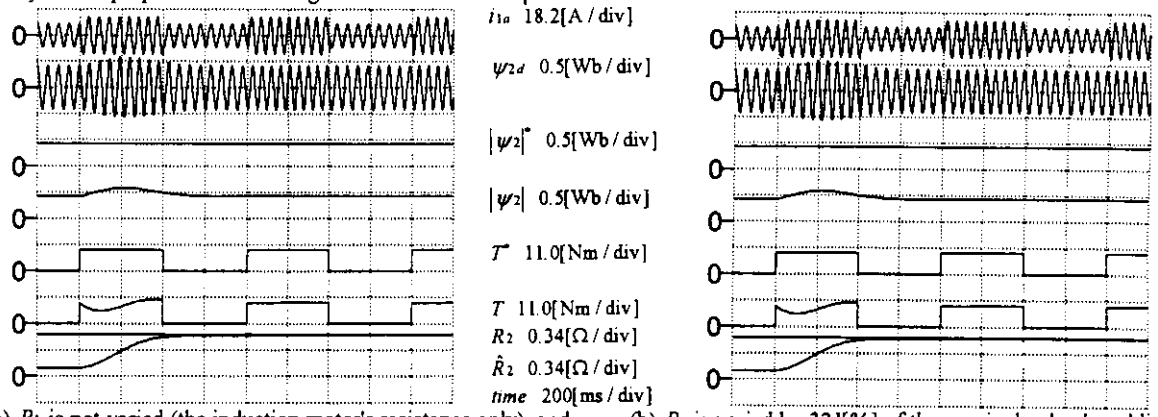

(a) R_1 is not varied (the induction motor's resistance only), and $\hat{R}_2$ is compensated.

(b) R_1 is varied by 321[%] of the nominal value by adding external resistances (1.2[Ω]), and $\hat{R}_2$ is compensated.

Fig. 6. Compensation characteristics of the secondary resistance variation (simulation results).

attained in Fig. 9(b). The value of $\hat{R}_2$ in this case was rather smaller than the nominal value. It is supposed that the nominal value included nearly 20[%] errors because it had been determined by using L-type equivalent circuit with thermal conversion. The torque response time was about 3[ms], and this performance was almost same as dc motor.

To verify the compensation characteristics of the secondary resistance variation, the output torque was controlled in the same way as shown in the simulation results. Figure 10 shows torque step responses of 100[%] torque, and torque reference was changed intermittently at low frequency (1.25[Hz]) for each test. The conditions are described in the captions of Fig. 10.

As shown in Figs. 10(a) and 10(b), the proposed control was essentially robust against the variation of R_1. Transient phenomena however, were measured in the torque responses because of the parameter mismatch of $\hat{R}_2$. The output torque was decreased by 57[%] in the steady state. On the other hand, improvement of the torque response was confirmed in Figs. 10(c) and 10(d). Transient phenomena in the responses were observed at the beginning of the $\hat{R}_2$ identification because its initial value had been set at 14[%] of the nominal value. The identification started automatically as the torque reference was stepped up, and $\hat{R}_2$ converged to a certain constant value in 400[ms]. The converged value conformed to the value that had been set so as to attain the optimal torque response in Fig. 9(b). Then the torque responses were improved without transient oscillations and steady-state errors. In addition to that, the variation of R_1 did not affect the compensation process as shown in Fig. 10(d).

Conclusions

The authors proposed a torque control strategy of the induction motor with robustness against the variations of the primary and the secondary resistances. In this paper, several results were obtained through the theoretical consideration, some digital simulations and experimental tests. The proposed technique is applicable to the flux-feedback-type torque control based on the primary or the secondary flux. The control is essentially robust against the variation of the primary resistance because its flux simulator employs a rotor current model. The variation of the secondary resistance however, affects strongly to the control performance. Introducing a robust secondary resistance identifier, its variation can be compensated completely without the effect of the primary resistance. The identifier is based on the instantaneous reactive power of the induction motor, and it can identify the secondary resistance value automatically and uniquely except the dc-exciting or no-load condition. The proposed technique is supposed to be more effective than conventional methods.

References

[1] F. Blaschke, "Das Prinzip der Feldorientierung, die Grundlage für die TRANSVEKTOR-Regelung von Drehfeldmaschinen," *Siemens Zeitschrift*, vol. 45, pp. 757-760, 1971

[2] A. Nabae, K. Otsuka, H. Uchino and R. Kurosawa, "An Approach

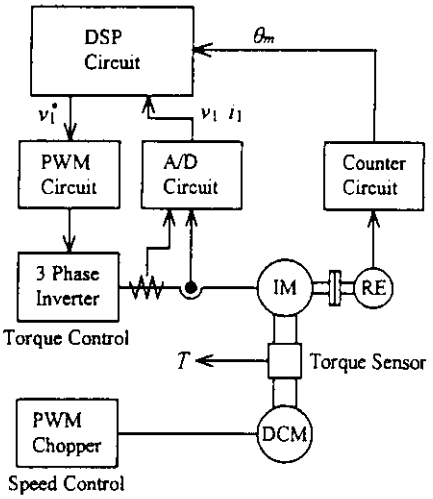

Fig. 7. Schematic diagram of the experimental system.

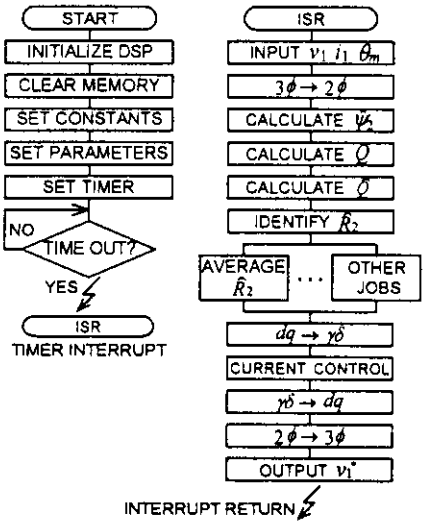

Fig. 8. Flow chart of DSP based control program.

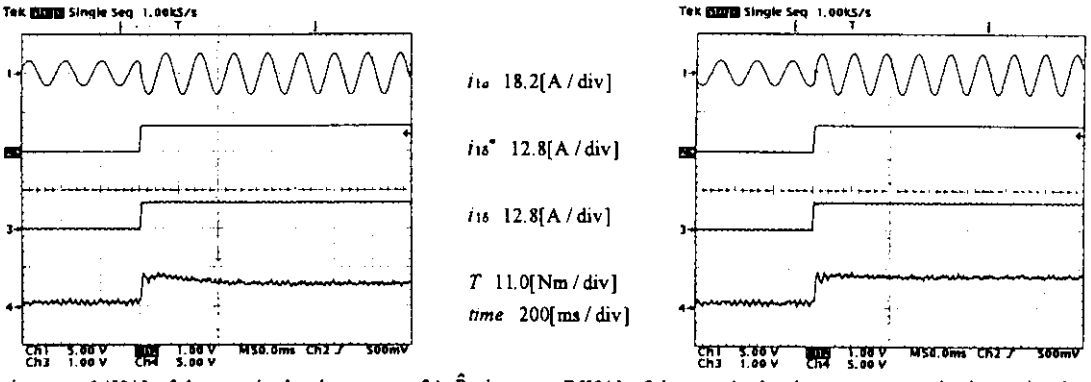

(a) $\hat{R}_2$ is set at 14[%] of the nominal value. (b) $\hat{R}_2$ is set at 76[%] of the nominal value so as to attain the optimal response.

Fig. 9. Characteristics of current and torque responses without compensation (experimental results).

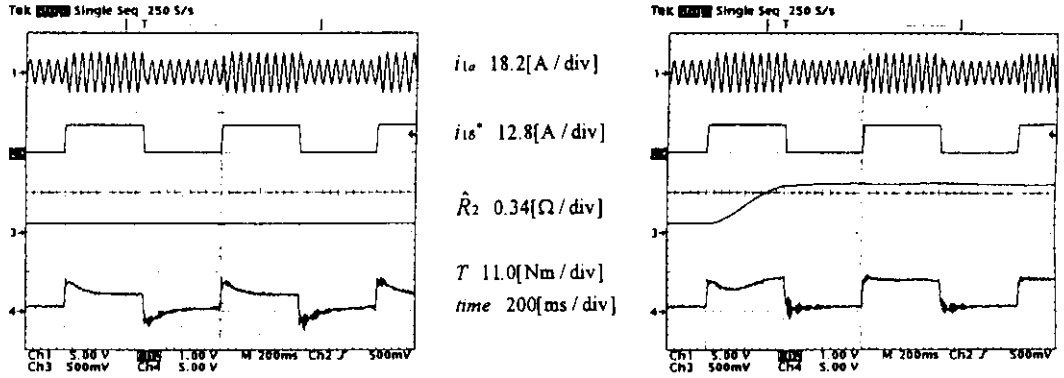

(a) R_1 is not varied (the induction motor's resistance only), and $\hat{R}_2$ has parameter mismatch by 14[%] of the nominal value.

(c) R_1 is not varied (the induction motor's resistance only), and $\hat{R}_2$ is compensated.

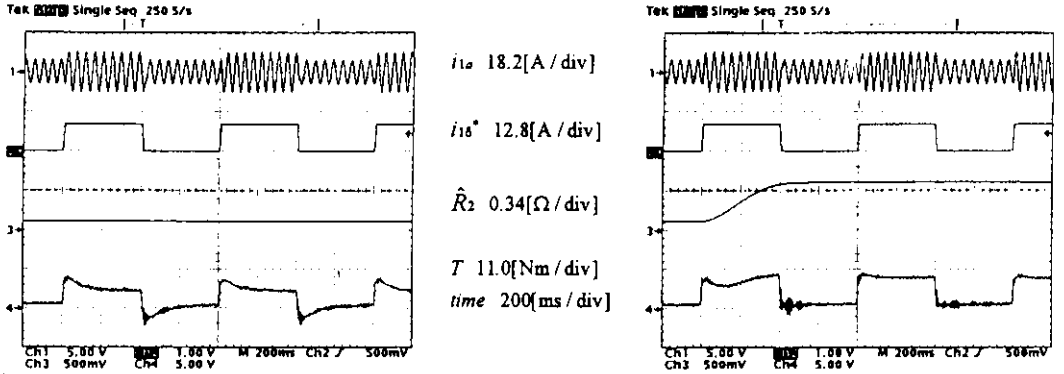

(b) R_1 is varied by 321[%] of the nominal value by adding external resistances (1.2[Ω]), and $\hat{R}_2$ has parameter mismatch by 14[%] of the nominal value.

(d) R_1 is varied by 321[%] of the nominal value by adding external resistances (1.2[Ω]), and $\hat{R}_2$ is compensated.

Fig. 10. Compensation characteristics of the secondary resistance variation (experimental results).

to Flux Control of Induction Motors Operated with Variable-Frequency Power Supply," *IEEE Trans. on Ind. App.*, vol. IA-16, no. 3, pp. 342-350, 1980

[3] R. Gabriel and W. Leonhard, "Microprocessor Control of Induction Motor," *IEEE ISPC Conf. Rec.*, pp. 385-395, 1982

[4] H. Sugimoto and S. Tamai, "Secondary Resistance Identification of an Induction Motor Applied Model Reference Adaptive System and Its Characteristics," *IEEE IAS Ann. Meet. Conf. Rec.*, pp. 613-620, 1985

[5] Y. Hori and T. Umeno, "Implementation of Robust Flux Observer Based Field Orientation (FOFO) Controller for Induction Machines," *IEEE IAS Ann. Meet. Conf. Rec.*, pp. 523-528, 1989

[6] J. Holtz and T. Thimm, "Identification of the Machine Parameters in a Vector Controlled Induction Motor Drive," *IEEE IAS Ann. Meet. Conf. Rec.*, pp. 601-606, 1989

[7] J. Moreira, K. Hung, T. Lipo and R. Lorenz, "A Simple and Robust Adaptive Controller for Detuning Correction in Field Oriented Induction Machines," *IEEE IAS Ann. Meet. Conf. Rec.*, pp. 397-403, 1991

[8] K. Tungpimolrut, F. Peng and T. Fukao, "Robust Vector Control of Induction Motor without Using Stator and Rotor Circuit Time Constants," *IEEE IAS Ann. Meet. Conf. Rec.*, pp. 521-527, 1993

[9] T. Noguchi, K. Yamada, S. Kondo and I. Takahashi, "Quick Torque Control of Induction Motor with Robustness against Variations of Primary and Secondary Resistances," *IEEJ Tech. Meet. on Static Power Converter*, SPC-94-92, pp. 77-86, 1994

[10] I. Takahashi and T. Noguchi, "A New Quick-Response and High-Efficiency Control Strategy of an Induction Motor," *IEEE Trans. on Ind. App.*, vol. IA-22, no. 5, pp. 820-827, 1986

Appendix

Effects of Inductance Mismatch on Identification

Assuming that there are parameter mismatches of not only the secondary resistance but also the inductance, the difference shown in Eq. (13) can be rewritten as follows:

$$\Delta Q = \frac{\omega\left\{M-\hat{M}+(\omega-\omega_m)^2\left(M\tau_2^2-\hat{M}\tau_2^2\right)\right\}}{\left\{1+(\omega-\omega_m)^2\hat{\tau}_2^2\right\}\left\{1+(\omega-\omega_m)^2\tau_2^2\right\}}|I_1|^2 \qquad \text{(A1)}$$

where $\tau_2 = L_{22}/R_2$ represents a secondary time constant, and it is supposed to be $L_{22} = M$. Letting $\omega - \omega_m \neq 0$, $\Delta M = \hat{M} - M$ and $\Delta\tau_2 = \hat{\tau}_2 - \tau_2$, the relation between ΔM and $\Delta\tau_2$ is expressed as shown below on condition that the identification has finished.

$$\Delta\tau_2 = \sqrt{\left(1+\frac{\Delta M}{M}\right)\tau_2^2+\frac{\Delta M}{(\omega-\omega_m)^2 M}} - \tau_2 \qquad \text{(A2)}$$

It is found that the identification error is affected by the parameter mismatch of the inductance. When the inductance of the motor decreases owing to magnetic saturation, which corresponds to the case of $\Delta M > 0$, $\Delta\tau_2$ increases approximately in proportion to ΔM. Additionally, $\Delta\tau_2$ becomes more sensitive to ΔM as a load is lighter. Therefore the parameter mismatch of the inductance should be reduced as precisely as possible.

Table 1. Nominal parameters and rated values of tested motor.

Rated output	1.5[kW]	L_{11}	55.17[mH]
Rated torque	8.63[Nm]	L_{22}	51.03[mH]
R_1	0.542[Ω]	M	51.03[mH]
R_2	0.536[Ω]	$\lvert\psi_2\rvert^*$	0.427[Wb]